RESEARCH PAPER

Acta Neurobiol Exp 2021, 81: 307–313
DOI: 10.55782/ane-2021-004

since 1928 ACTA NEUROBIOLOGIÆ EXPERIMENTALIS

Annexin A3: a newly identified player in store-operated calcium entry

Agnieszka Dyrda, Jacek Kuznicki and Lukasz Majewski*

Laboratory of Neurodegeneration, International Institute of Molecular and Cell Biology, Warsaw, Poland,
** Email: lmajewski@iimcb.gov.pl*

Store-operated calcium entry (SOCE) is important for refilling endoplasmic reticulum (ER) Ca^{2+} stores and Ca^{2+} signaling. Extracellular Ca^{2+} is conducted by highly Ca^{2+}-selective Orai channels that are activated by stromal interaction molecule proteins (STIMs), which are sensitive ER Ca^{2+} sensors. We found an approximately five-fold increase in *annexin A3a* (*anxa3*a) expression levels in *stim2b* knockout zebrafish. The present study investigated whether annexin A3 protein is involved in SOCE. We used Ca^{2+} imaging and electrophysiological recordings to determine the effect of annexin A2, A3, and A6 overexpression on SOCE and Orai-dependent Ca^{2+} currents (ICRAC) in cultured cells. Annexin A3 increased SOCE amplitude and potentiated Ca^{2+} I_{CRAC} currents. These results suggest that annexin A3 is a positive modulator of SOCE.

Key words: *anxa3a*, annexin A3, store-operated calcium entry, calcium homeostasis

INTRODUCTION

Stromal interaction molecule 1 (STIM1) and STIM2 are endoplasmic reticulum (ER) Ca^{2+} sensors that contain two EF-hand motifs (Williams et al., 2001; Liou et al., 2005; Roos et al., 2005; Parvez et al., 2008). Following Ca^{2+} release from the ER that is triggered by agonists and mediated by inositol-1,4,5-trisphosphate receptors, STIMs participate in ER Ca^{2+} refilling by activating highly Ca^{2+}-selective Orai1-3 channels that are located in the plasma membrane (Mercer et al., 2006; DeHaven et al., 2007; Lis et al., 2007). Based on the electrochemical gradient across the plasma membrane, extracellular Ca^{2+} flows into the cytosol and is pumped into the ER by Ca^{2+}-adenosine triphosphatase. This process is known as store-operated calcium entry (SOCE) (Baba et al., 2006; Spassova et al., 2006). Ca^{2+} currents that flow through Orai channels are gated by STIM proteins, referred to as calcium release-activated calcium (CRAC, I_{CRAC}) currents. STIM and Orai proteins are present in virtually every cell type. SOCE is a common and basic physiological mechanism, including skeletal muscles and neurons (Kraft, 2015; Majewski and Kuznicki, 2015; Wegierski and Kuznicki, 2018).

Various proteins have been identified as modulators of SOCE (recently summarized in Berlansky et al., 2021), and this list of proteins is expanding. Importantly, not all of these proteins play a role via direct interactions with STIM or Orai. Monastyrskaya et al. (2009) overexpressed fluorescent protein-tagged annexin A1 (AnxA1), AnxA2, and AnxA6 in HEK293 cells using H- and K-Ras membrane anchors and found that AnxA6 affected SOCE amplitude. Nishiura et al. (2014) reported that AnxA3 in the human HL-60 promyeloblast cell line bound to plasma membrane phospholipids in a Ca^{2+}-dependent manner and regulated Ca^{2+} oscillations that were sensitive to a SOCE inhibitor.

Humans express 12 different Anxs (AnxA1-11 and AnxA13), which have orthologs in most vertebrates. To belong to the Anx family, a protein must fulfill two major criteria: should bind to negatively charged phospholipids in a Ca^{2+}-dependent manner and should contain a conserved structural element,

Received 16 November 2021, accepted 4 December 2021

the so–called annexin repeat. The intracellular localization of Anxs is highly variable, from the soluble cytoplasmic pool to the cell surface. Anxs reversibly bind to negatively charged phospholipids. Among different anionic phospholipids, Anxs display a marked preference for phosphatidylserine (PS) over phosphatidylethanolamine (PE). Additionally, Anxs bind other phospholipidic components of the intracellular leaflet: phosphatidic acid (PA), phosphatidylglycerol (PG) or phosphatidylinositol (PI). Some Anxs feature more specific interactions with membrane lipids. AnxA2 and AnxA8, for example, bind phosphatidylinositol-4,5-bisphosphate (PIP2) (Rescher et al., 2004; Goebeler et al., 2006; Hayes et al., 2009) and AnxA3 was recently shown to be one of the highly abundant protein in membrane-derived exosomes enriched in sphingomyelin (Dang et al., 2017). The wide range of Ca^{2+} affinities (KD≈25-1000 μM, except for AnxA6 whose KD is ≈1 μM) suggests that particular members of the Anx family may respond differently to changes in cytosolic [Ca^{2+}] (Domon et al., 2013; Veschi et al., 2020). That also hints that Anxs translocate from cytosol to the membrane only at certain, well-defined amplitude of the stimuli (Gerke et al., 2005). As membrane-membrane and membrane-cytoskeletal linkers, Anxs reversibly associate with components of the cytoskeleton or other proteins. Although studied for over four decades, the precise physiological role of Anxs is far from being understood.

Our laboratory recently showed that *stim2b*$^{-/-}$ zebrafish larvae exhibited neurological symptoms 5 days postfertilization (dpf) (Wasilewska et al., 2020). The *stim2b*$^{-/-}$ mutants were hyperactive, indicated by increases in mobility and thigmotaxis and the disruption of phototaxis in the light/dark preference test. Compared with wildtype (WT) fish, the frequency and amplitude of neuronal Ca^{2+} oscillations increased in optic tectum neurons (Wasilewska et al., 2020). RNA sequencing (RNAseq) revealed the upregulation of several genes, including *anxa3a*, which was the most upregulated (five-fold increase) compared with WT fish. This observation and previous findings by Nishiura et al. (2014) prompted us to study the role of AnxA3 in SOCE. The present study performed Ca^{2+} imaging and electrophysiological methods and found that AnxA3 is a positive modulator of SOCE.

METHODS

Materials

Cyclopiazonic acid (CPA) was obtained from Sigma (catalog no. C1530). Thapsigargin was obtained from HelloBio (catalog no. HB1118). Fura-2 AM was obtained from Life Technologies (catalog no. F1221). Pluronic F-127 was obtained from Invitrogen (catalog no. P6867). All other compounds for solution preparation were analytical grade and purchased from Sigma, Fluka, or BioShop.

Cell culture and transfections

The human embryonic kidney 293T (HEK293T) cell line (American Type Culture Collection: CRL-11268, lot no. 59587035) and HeLa cell line were maintained in Dulbecco's Modified Eagle Medium (Sigma, catalog no. D6426) supplemented with 1% penicillin/streptomycin (Gibco, catalog no. 15140) and 10% fetal bovine serum (Sigma, catalog no. F9665). The cells were passaged every 4 days and used until passage 30 to avoid changes in cell phenotypes (Thomas and Smart, 2005; Kurejova et al., 2007). Twenty-four hours before the experiments, the cells were transiently co-transfected with PEI 25K, a linear polyethyleneimine (Polysciences, catalog no. 23966), according to the manufacturer's instructions. For the electrophysiological experiments with HEK293T cells, the cells were transfected with Orai1-Myc and STIM1-yellow fluorescent protein (YFP) at a 1:2 (Orai:STIM) molar DNA ratio, and Orai1-Myc, STIM1-YFP, and AnxA3-mCherry were overexpressed at 1:2:1 (Orai:STIM:AnxA) molar DNA ratio. Table 1 presents a list of plasmid sources.

Table 1. Plasmid sources.

Plasmid	Source
AnxA2	Marta Miaczynska laboratory
AnxA3	GeneCopoeia (catalog no. EX-T0388-M56)
AnxA6	Volker Gerke laboratory
Orai1-Myc (Cterm)	Addgene (catalog no. 21638)
STIM1-YFP (Cterm)	Jacek Kuznicki laboratory (unpublished)

Zebrafish lines and maintenance

Wildtype, *stim2b*$^{-/-}$, *stim2a*$^{-/-}$, and *stim2ab*$^{-/-}$ zebrafish were used in the study. The generation of the mutant zebrafish lines was described previously (Gupta et al., 2020; Wasilewska et al., 2020). The fish were maintained according to previously described protocols (Matthews et al., 2002) in the Zebrafish Core Facility (PL14656251, registry of the District Veterinary Inspectorate in Warsaw; 064 and 051, registry of the Ministry of Science and Higher Education) at the International Institute of Molecular and Cell Biology in Warsaw. All experiments with zebrafish larvae were performed in accordance with the European Communities Council Directive (63/2010/EEC). The larvae were kept in E3 medium (2.48 mM NaCl, 0.09 mM KCl, 0.164 mM $CaCl_2{\cdot}2H_2O$, and 0.428 mM $MgCl_2{\cdot}6H2O$) at 28.5°C. The larvae were kept in a Petri dish (~50 larvae/dish) in an incubator under a 14 h/10 h light/dark cycle.

Quantitative polymerase chain reaction gene expression analysis

RNA isolation and cDNA synthesis were performed as previously described (Wasilewska et al., 2020). Data were analyzed using Bio-Rad CFX Maestro 1.0 software. Specificity of the reaction was determined by dissociation curve analysis. Fold changes were calculated using the ΔΔCq method as previously described (Majewski et al., 2019). The 18*S* ribosomal gene and eukaryotic translation elongation factor 1 α1, like 1 (*eef1a1l1*) gene were used as a reference. The following primer sets were used in the analysis: anxa3a_e4/5-e6 (forward: TGAAGGCGTTGGTACAAATGAA; reverse: CCATGGGTCTCGCCTTTCAA), anxa3b_e9-11 (forward: AATGTGGACGTGGCAAAAGC; reverse: TTCCTGAAGGGTTCTTCCGC), anxa5a_e5/6-e7 (forward: AGGCTATCAAGGGAGTGGGT, reverse: TCTTCACATGTCCTGGACG), and anxa1c_e1-e1/2 (forward: CAAAGTTTGCAAGATGGCCTTT, reverse: GAGCAGCTTTAAAACCCGTG).

Ca^{2+} measurements

For cytosolic Ca^{2+} measurements, HeLa cells were loaded with 2 μM Fura-2 AM and 0.1% pluronic acid (Pluronic F-127) in the dark at room temperature for 45 min in a Ca^{2+}-containing solution and washed twice. Intracellular de-esterification of the dye was allowed for 20 min. Fluorescence was recorded using an Olympus IX81 microscope (20'/0.75 UPLSAPO objective) that was equipped with a MT20 illumination system that rapidly changed excitation wavelengths between 340 and 380 nm (ET340x and ET380x filters, respectively; Chroma). Emission was collected by a cooled EM-CCD camera (Hamamatsu) through a T400LP dichroic mirror and an ET510/80 filter (Chroma). Images were acquired using CellR software (Olympus), and the analysis was performed using ImageJ software (Schneider et al., 2012). Cells were stimulated with 20 μM CPA in Ca^{2+}-free solution for 10 min, and then 2 mM Ca^{2+} in the presence of 20 μM CPA was added to reveal SOCE. The solution contained 140 mM NaCl, 5 mM KCl, 1 mM $MgCl_2$, 20 mM HEPES, 10 mM glucose, and 2 mM $CaCl_2$ in Ca^{2+}-containing solution or 1 mM ethylene glycol-bis(β-aminoethyl ether)-*N*,*N*,*N'*,*N'*-tetraacetic acid (EGTA) without Ca^{2+} in Ca^{2+}-free solution, pH 7.4 (NaOH).

Electrophysiology

Patch-clamp recordings were performed in whole-cell mode using electrodes with resistances between 3.0 and 4.0 MΩ. The electrodes were pulled from 1.5 mm thin-wall glass capillaries (Science Products, catalog no. GB150F-10P) using a horizontal Sutter instrument puller (model P-1000). The pipette solution contained 125 mM cesium methansulfonate, 10 mM CsCl, 8 mM $MgCl_2$, 10 mM HEPES, 10 mM 1,2-bis(*O*-amino phenoxy)ethane-*N*,*N*,*N'*,*N'*-tetraacetic acid (BAPTA), and 0.001 mM thapsigargin, pH 7.2 (CsOH). The extracellular solution contained 135 mM NaCl, 10 mM CsCl, 4.4 mM $MgCl_2$, 2.8 mM KCl, 10 mM HEPES, 0.5 mM ethylenediaminetetraacetic acid (EDTA), 0.5 mM EGTA, 10 mM glucose, and 11 mM $CaCl_2$ (free Ca^{2+} 10 mM), pH 7.4 (NaOH). For the "0 mM" $CaCl_2$ solution, no Ca^{2+} was added, and the NaCl concentration was increased to 145 mM. After establishing whole-cell mode, HEK293T cells were left for a minimum of 3 min in the absence of extracellular Ca^{2+} before adding 10 mM $CaCl_2$. Gd^{3+} (10 μM) was added at the end of recording to block currents and estimate leak currents. Currents were recorded during a 300 ms ramp of potentials, ranging from -130 mV to +85 mV, applied every 5 s, with Axon pCLAMP 11 Electrophysiology Data Acquisition and Analysis software (Molecular Devices) using a Multiclamp 700B Amplifier (Axon; Molecular Devices), low-pass filtered at 1 kHz, and digitized with Digidata 1550B. For each time point, currents at -100 mV and +80 mV were plotted over time.

Statistical analysis

For each dataset, the statistical tests that were used to determine significant differences are presented in the figure legends.

RESULTS

stim2 knockout in zebrafish increases *anxa3a* expression

Our laboratory recently reported alterations of Ca^{2+} oscillations in neurons in *stim2b*$^{-/-}$ zebrafish (Wasilewska et al., 2020). The *stim2* gene is duplicated in zebrafish (*Danio rerio*). Therefore, two other mutants were generated: *stim2a*$^{-/-}$ and *stim2a*$^{-/-}$/*stim2b*$^{-/-}$ (stim2ab$^{-/-}$) double knockout. Quantitative polymerase chain reaction (qPCR) analysis confirmed our earlier RNAseq analysis (Wasilewska et al., 2020), in which *anxa3a* expression was significantly upregulated in *stim2b*$^{-/-}$ larvae 5 dpf (Fig. 1). Similar upregulation of *anxa3a* expression was detected in *stim2ab*$^{-/-}$ mutants (Fig. 1). However, in *stim2a*$^{-/-}$ fish, *anxa3a* expression was not significantly different form WT controls (Fig. 1).

The expression levels of *anxa1c*, *anxa3b*, and *anxa5a* did not significantly change in any of the mutant lines compared with WT larvae (Fig. 1). Thus, following *stim2* downregulation, only *anxa3a* expression was specifically upregulated.

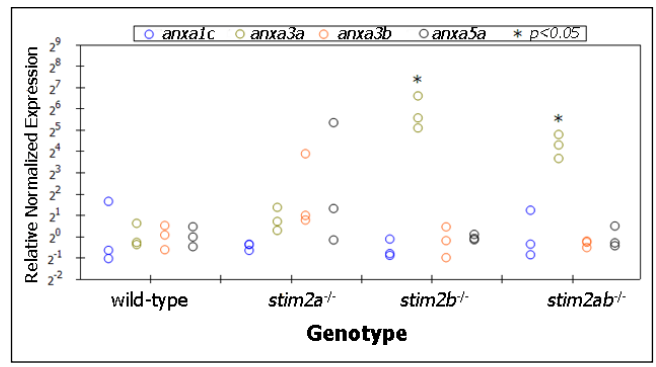

Fig. 1. Expression profiles of selected *anxs* in 5 dpf larvae (wildtype and *stim2a*$^{-/-}$, *stim2b*$^{-/-}$, and *stim2ab*$^{-/-}$ knockout) analyzed by qPCR. The results are shown as dot plots. Each circle represents one sample from one fish. The results showed the upregulation of *anxa3a* gene expression. The data are expressed as a fold change ($2^{-\Delta\Delta Ct}$) that was normalized to the reference gene. *p<0.05 (Tukey's *post hoc* test; CFX software [Bio-Rad]).

Annexin A3 increases SOCE amplitude

STIM proteins initiate Ca^{2+} influx in SOCE. We previously found alterations of Ca^{2+} oscillations in *stim2b*$^{-/-}$ zebrafish neurons (Wasilewska et al., 2020). In the present study, we investigated whether SOCE amplitude is altered in the presence of AnxA3 (Fig. 2).

HeLa cells were transiently overexpressed with fluorescently tagged AnxA3, which is a mammalian homolog of *anxa3a* in *Danio rerio*. Two other fluorescently labeled annexins, AnxA2 and AnxA6, were used for comparison. Fig. 2A shows the mean traces of SOCE with the readdition of Ca^{2+} in non-transfected and AnxA2-, AnxA3-, and AnxA6-overexpressing HeLa cells. SOCE amplitudes were estimated from the Ca^{2+} readdition step (Fig. 2B).

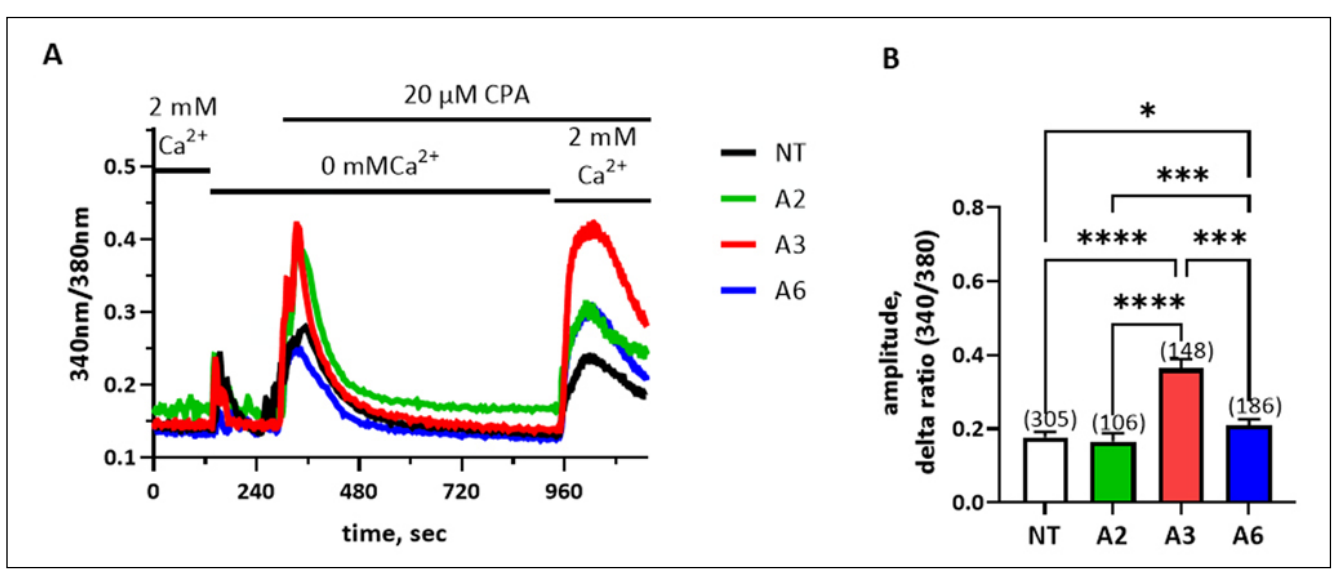

Fig. 2. Overexpression of AnxA3 increases SOCE Ca^{2+} amplitude. HeLa cells were transiently transfected with AnxA2-mCherry (A2), AnxA3-mCherry (A3), or AnxA6-eGFP (A6) constructs. Cytosolic Ca^{2+} concentrations were monitored by ratiometric Ca^{2+}-sensitive Fura-2AM dye, and SOCE was activated with 20 µM CPA. (A) Mean traces of SOCE amplitude with the readdition of Ca^{2+} in non-transfected (NT) and AnxA2 (A2)-, AnxA3 (A3), and AnxA6 (A6)-overexpressing HeLa cells. Error bars are omitted in the figure for the sake of clarity. (B) SOCE amplitudes estimated at the Ca^{2+} readdition step in CPA-treated cells. Numbers in parentheses indicate the total number of cells that were analyzed from a minimum three independent transfections. The data are expressed as mean ± SEM. *p<0.05, ***p<0.001, ****p<0.0001 (Kruskal-Wallis one-way analysis of variance follow by Dunn's *post hoc* test).

As documented previously (Wegierski et al., 2016; Albarran et al., 2018), SOCE is present in non-transfected HeLa cells. The overexpression of AnxA2 did not change SOCE amplitudes compared with non-transfected cells. The overexpression of either AnxA3 or AnxA6 significantly increased SOCE amplitudes. In the presence of AnxA3, however, this SOCE amplitude potentiation reached higher statistical power. Altogether, this experiment showed that AnxA3 can amplify SOCE amplitudes.

Annexin A3 increases CRAC amplitude

Although Fura2-based Ca^{2+} measurements are useful for estimating SOCE amplitudes, a major drawback of this technique is the lack of information about which types of channels participate in the process. To discriminate which channels are affected by the presence of AnxA3 in SOCE measurements (i.e., highly Ca^{2+} selective Orai channels or nonselective cationic transient receptor potential channels [TRPCs]), the electrophysiological patch-clamp technique was used. The signature of prototypical CRAC (I_{CRAC}) currents is an inwardly rectifying current to voltage (I/V) relationship. I_{CRAC} is a Ca^{2+} current that is mediated by Orai1 channels that are activated by STIM1 following ER Ca^{2+} store deprivation; thus, its reversal potential (E_{rev}) is highly positive (> +80 mV). We compared two currents: I_{CRAC} activated in HEK cells that were transiently transfected with Orai1 and STIM1 (O1+S1) and I_{CRAC} activated in HEK cells that were transiently transfected with Orai1, STIM1, and AnxA3 (O1+S1+A3). Representative I_{CRAC} development is shown in Fig. 3A.

The positive and negative potentials were chosen to monitor outward and inward currents, respectively. To generate the I/V curve, the sweep with the most negative value of the current at -100 mV of the imposed membrane potential was selected. Fig. 3B shows the mean ± SEM I/V curves that were recorded for cells that overexpressed Orai1 and STIM1 (O1+S1, black points) and Orai1+STIM1+AnxA3 (O1+S1+A3, red points). Both I/V curves resembled prototypical I_{CRAC} I/V curves (i.e., inwardly rectifying and highly positive E_{rev}). Capacitive current values at -100 mV of the imposed membrane potentials were significantly more negative for cells that expressed AnxA3 than for cells that expressed only Orai1 and STIM1. This indicates that I_{CRAC} was potentiated in the presence of AnxA3 (Fig. 3B), which might explain the higher SOCE amplitude in the Ca^{2+} Fura-2AM measurements.

DISCUSSION

The hypothesis that AnxA3 might be involved in Ca^{2+} homeostasis is based on recent data from our group (Wasilewska et al., 2020), in which *anxa3a* expression was upregulated as a result of *stim2b* knockout in zebrafish, determined by RNAseq analysis. In the present study, we used qPCR to confirm that only *anxa3a* expression increased, with no changes in *anxa1c*, *anxa3b*, or *anxa5a* expression. Consistent with this observation was the increase in *anxa3a* expression in *stim2ab*$^{-/-}$ ze-

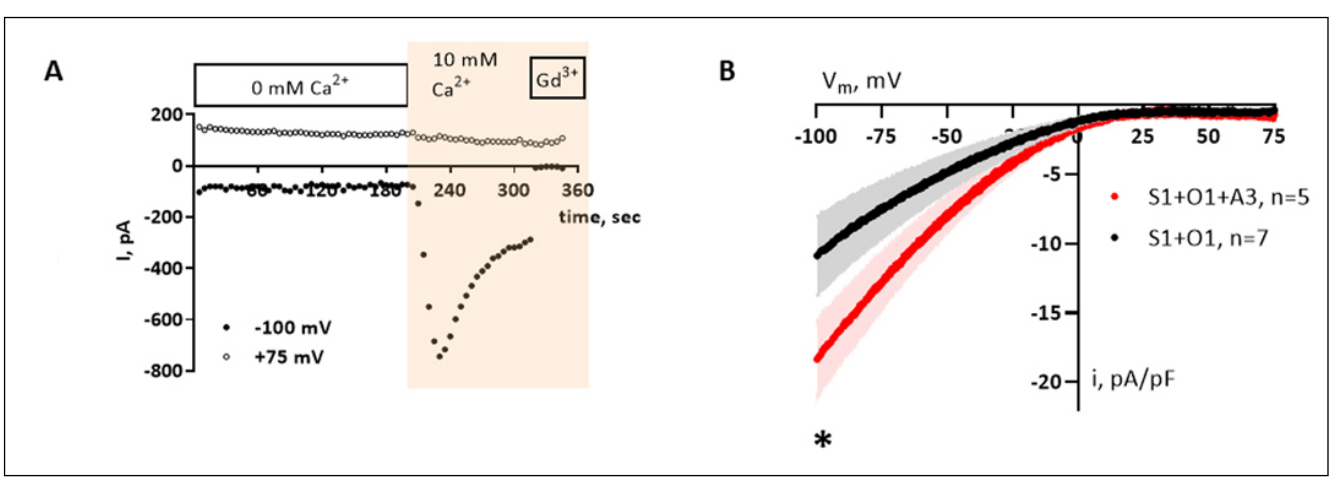

Fig. 3. AnxA3 increases CRAC current amplitude. Cells were transfected with STIM1-YFP and Orai1-Myc (S1+O1) or STIM1-YFP, Orai1-Myc, and AnxA3-mCherry (S1+O1+A3). The protocol to activate SOCE currents was applied as described in the Materials and Methods section. Current amplitudes at -100 mM and +75 mV were chosen to monitor inward and outward currents, respectively. (A) Representative traces of I_{CRAC} development. (B) The black and red I/V curves (mean ± SEM) show currents that were recorded in S1+O1 and S1+O1+A3 expressing cells, respectively. The I_{CRAC} current amplitude measured at -100 mV increased in cells that expressed AnxA3. The numbers (*n*) of patch-clamped cells are shown in the figure. **p*<0.05 (unpaired *t*-test with Welch's correction).

brafish. Interestingly, knocking out only *stim2a* (*stim2a*$^{-/-}$ zebrafish) did not alter the expression of any of the annexin genes tested. This might indicate that *stim2a* and *stim2b* genes have different functions, similar to STIM isoforms in mammalian cells (Gruszczynska-Biegala et al., 2011; Miederer et al., 2015; Ramesh et al., 2021).

We found that SOCE amplitudes significantly increased in AnxA3-expressing HeLa cells compared with control cells. As expected, AnxA2 overexpression did not alter SOCE amplitudes. In contrast to the previously published results (Monastyrskaya et al., 2009), however, the overexpression of AnxA6 did not decrease and instead increased SOCE amplitudes but to lesser extent than AnxA3 did. The reason for these disparate results with regard to the effects of AnxA6 on SOCE amplitudes is unclear. Monastyrskaya et al. (2009) activated SOCE using thapsigargin, whereas we used CPA. Whether specific type of agent that depletes Ca2+ stores has an effect on Anxs and, indirectly, influence Anxs' action on SOCE amplitudes, requires further examination. Other differences between these studies include transfection with constructs that encode Anxs without providing targeting sequences versus constructs that encode Anxs with a plasma membrane anchor and the types of cells that were analyzed (HeLa cells in the present study and HEK293 cells in the previous study (Monastyrskaya et al., 2009). Another possibility might originate from the distinct structure of Anxs, which possess a different number of Ca^{2+} binding domains as well as unique interaction partners, e.g., AnxaA2 may bind with the S100 family proteins (MacLeod et al., 2003; Bandorowicz-Pikula et al., 2012; Weisz and Uversky, 2020).

Our electrophysiological patch-clamp recordings in HEK293 cells that overexpressed AnxA3 demonstrated the potentiation of Orai-dependent I_{CRAC} currents. This would strongly suggest that also in our calcium imaging experiments, the augmented Ca^{2+} amplitude is most probably due to an increase Orai-dependent Ca^{2+} entry than to activity of the other Ca^{2+} entry pathway(s). We only examined the combination of Orai1 and STIM1, but our zebrafish data implicate the STIM2 isoform is also important. Further studies are needed to examine how the observed effects on I_{CRAC} current amplitudes are influenced by other known Orai and STIM isoforms (DeHaven et al., 2007; Lis et al., 2007). As described by others, they are known to have distinguishable effects on SOCE (Miederer et al., 2015; Vaeth et al., 2017). Additionally, it is important to determine how stoichiometric ratios of AnxA3, Orais, and STIMs can affect the modulation of SOCE. Moreover, we cannot exclude the possibility that AnxA3 interacts with other ion transporters, especially nonselective canonical channels (e.g., TRPCs) that have been shown to participate in SOCE (Huang et al., 2006; Liao et al., 2008; Zeng et al., 2008; Lee et al., 2010; Hartmann et al., 2014; Zhang et al., 2016; Dyrda et al., 2020).

CONCLUSIONS

Despite the considerable progress in developing biochemical and molecular biology tools and many studies, the exact functions of individual Anxs still await clarifications. Given the broad spectrum of physiological processes in which Anxs are involved (including Ca^{2+} signaling), it is surprising and somewhat unexpected to see the small number of publications in which these Ca^{2+}-dependent proteins have been studied together with or in the context of SOCE. The present study merged research on SOCE and Anxs by providing evidence that AnxA3 influences SOCE processes. We think that *stim2* KO zebrafish model overexpressing AnxA3 will help us learn more about the function of Anxs in Ca^{2+} homeostasis and signaling. Changes in neuronal Ca^{2+} oscillations and behavior in the *stim2* KO zebrafish model are an exciting line of further exploration.

ACKNOWLEDGEMENTS

We thank Dr. Tomasz Wegierski for providing the construct that was used in this study and useful discussions and comments on the manuscript. We thank Prof. Marta Miaczynska (International Institute of Molecular and Cell Biology in Warsaw, Poland) for providing the AnxA2 construct and Prof. Volker Gerke (University of Münster, Germany) for providing the AnxA6 construct. This work was funded by the National Science Centre (grant no. 2016/23/B/NZ3/03142) to JK.

REFERENCES

Albarran L, Lopez JJ, Jardin I, Sanchez-Collado J, Berna-Erro A, Smani T, et al. (2018) EFHB is a novel cytosolic Ca2+ sensor that modulates STIM1-SARAF interaction. Cell Physiol Biochem 51: 1164–1178.

Baba Y, Hayashi K, Fujii Y, Mizushima A, Watarai H, Wakamori M, et al. (2006) Coupling of STIM1 to store-operated Ca2+ entry through its constitutive and inducible movement in the endoplasmic reticulum. Proc Natl Acad Sci U S A 103: 16704–16709.

Bandorowicz-Pikula J, Wos M, Pikula S (2012) Do annexins participate in lipid messenger mediated intracellular signaling? A question revisited. Mol Membr Biol 29: 229–242.

Berlansky S, Humer C, Sallinger M, Frischauf I (2021) More than just simple interaction between STIM and orai proteins: CRAC channel function enabled by a network of interactions with regulatory proteins. Int J Mol Sci 22: 471.

Dang VD, Jella KK, Ragheb RRT, Denslow ND, Alli AA (2017) Lipidomic and proteomic analysis of exosomes from mouse cortical collecting duct cells. FASEB J 31: 5399–5408.

DeHaven WI, Smyth JT, Boyles RR, Putney JW Jr (2007) Calcium inhibition and calcium potentiation of Orai1, Orai2, and Orai3 calcium release-activated calcium channels. J Biol Chem 282: 17548–17556.

Domon MM, Besson F, Tylki-Szymanska A, Bandorowicz-Pikula J, Pikula S (2013) Interaction of AnxA6 with isolated and artificial lipid microdomains; importance of lipid composition and calcium content. Mol Biosyst 9: 668–676.

Dyrda A, Koenig S, Frieden M (2020) STIM1 long and STIM1 gate differently TRPC1 during store-operated calcium entry. Cell Calcium 86: 102134.

Gerke V, Creutz CE, Moss SE (2005) Annexins: linking Ca2+ signalling to membrane dynamics. Nat Rev Mol Cell Biol 6: 449–461.

Goebeler V, Ruhe D, Gerke V, Resche, U (2006) Annexin A8 displays unique phospholipid and F-actin binding properties. FEBS Lett 580: 2430–2434.

Gruszczynska-Biegala J, Pomorski P, Wisniewska MB, Kuznicki J (2011) Differential roles for STIM1 and STIM2 in store-operated calcium entry in rat neurons. PLoS One 6: e19285.

Gupta RK, Wasilewska I, Palchevska O, Kuznicki J (2020) Knockout of stim2a Increases calcium oscillations in neurons and induces hyperactive-like phenotype in zebrafish larvae. Int J Mol Sci 21: 6198.

Hartmann J, Karl RM, Alexander RPD, Adelsberger H, Brill MS, Ruhlmann C, et al. (2014) STIM1 controls neuronal Ca2+ signaling, mGluR1-dependent synaptic transmission, and cerebellar motor behavior. Neuron 82: 635–644.

Hayes MJ, Shao DM, Grieve A, Levine T, Bailly M, Moss SE (2009) Annexin A2 at the interface between F-actin and membranes enriched in phosphatidylinositol 4,5,-bisphosphate. Biochim Biophys Acta 1793: 1086–1095.

Huang GN, Zeng W, Kim JY, Yuan JP, Han L, Muallem S, et al. (2006) STIM1 carboxyl-terminus activates native SOC, I(crac) and TRPC1 channels. Nat Cell Biol 8: 1003–1010.

Kraft R (2015) STIM and ORAI proteins in the nervous system. Channels 9: 245–252.

Kurejova M, Uhrik B, Sulova Z, Sedlakova B, Krizanova O, Lacinova L (2007) Changes in ultrastructure and endogenous ionic channels activity during culture of HEK 293 cell line. Eur J Pharmacol 567: 10–18.

Lee KP, Yuan JP, So I, Worley PF, Muallem S (2010) STIM1-dependent and STIM1-independent function of transient receptor potential canonical (TRPC) channels tunes their store-operated mode. J Biol Chem 285: 38666–38673.

Liao Y, Erxleben C, Abramowitz J, Flockerzi V, Zhu MX, Armstrong DL, et al. (2008) Functional interactions among Orai1, TRPCs, and STIM1 suggest a STIM-regulated heteromeric Orai/TRPC model for SOCE/Icrac channels. Proc Natl Acad Sci U S A 105: 2895–2900.

Liou J, Kim ML, Heo WD, Jones JT, Myers JW, Ferrell JE Jr, et al. (2005) STIM is a Ca2+ sensor essential for Ca2+-store-depletion-triggered Ca2+ influx. Curr Biol 15: 1235–1241.

Lis A, Peinelt C, Beck A, Parvez S, Monteilh-Zoller M, Fleig A, et al. (2007) CRACM1, CRACM2, and CRACM3 are store-operated Ca2+ channels with distinct functional properties. Curr Biol 17: 794–800.

MacLeod TJ, Kwon M, Filipenko NR, Waisman DM (2003) Phospholipid-associated annexin A2-S100A10 heterotetramer and its subunits: characterization of the interaction with tissue plasminogen activator, plasminogen, and plasmin. J Biol Chem 278: 25577–25584.

Majewski L, Kuznicki J (2015) SOCE in neurons: Signaling or just refilling? Biochim Biophys Acta 1853: 1940–1952.

Majewski L, Wojtas B, Maciag F, Kuznicki J (2019) Changes in calcium homeostasis and gene expression implicated in epilepsy in hippocampi of mice overexpressing ORAI1. Int J Mol Sci 20: 5539.

Matthews M, Trevarrow B, Matthews J (2002) A virtual tour of the Guide for zebrafish users. Lab Anim 31: 34–40.

Mercer JC, Dehaven WI, Smyth JT, Wedel B, Boyles RR, Bird GS, et al. (2006) Large store-operated calcium selective currents due to co-expression of Orai1 or Orai2 with the intracellular calcium sensor, Stim1. J Biol Chem 281: 24979–24990.

Miederer AM, Alansary D, Schwar G, Lee PH, Jung M, Helms V, et al. (2015) A STIM2 splice variant negatively regulates store-operated calcium entry. Nat Commun 6: 6899.

Monastyrskaya K, Babiychuk EB, Hostettler A, Wood P, Grewal T, Draeger A (2009) Plasma membrane-associated annexin A6 reduces Ca2+ entry by stabilizing the cortical actin cytoskeleton. J Biol Chem 284: 17227–17242.

Nishiura H, Yamanegi K, Kawabe M, Kato-Kogoe N, Yamada N, Nakasho K (2014) Annexin A3 plays a role in cytoplasmic calcium oscillation by extracellular calcium in the human promyelocytic leukemia HL-60 cells differentiated by phorbol-12-myristate-13-acetate. Exp Mol Pathol 97: 241–246.

Parvez S, Beck A, Peinelt C, Soboloff J, Lis A, Monteilh-Zoller M, et al. (2008) STIM2 protein mediates distinct store-dependent and store-independent modes of CRAC channel activation. FASEB J 22: 752–761.

Ramesh G, Jarzembowski L, Schwarz Y, Poth V, Konrad M, Knapp ML, et al. (2021) A short isoform of STIM1 confers frequency-dependent synaptic enhancement. Cell Rep 34: 108844.

Rescher U, Ruhe D, Ludwig C, Zobiack,N, Gerke V (2004) Annexin 2 is a phosphatidylinositol (4,5)-bisphosphate binding protein recruited to actin assembly sites at cellular membranes. J Cell Sci 117: 3473.

Roos J, DiGregorio PJ, Yeromin AV, Ohlsen K, Lioudyno M, Zhang S, et al. (2005) STIM1, an essential and conserved component of store-operated Ca2+ channel function. J Cell Biol 169: 435–445.

Schneider CA, Rasband WS, Eliceiri KW (2012) NIH Image to ImageJ: 25 years of image analysis. Nat Methods 9: 671–675.

Spassova MA, Soboloff J, He LP, Xu W, Dziadek MA, Gill, DL (2006) STIM1 has a plasma membrane role in the activation of store-operated Ca(2+) channels. Proc Natl Acad Sci U S A 103: 4040–4045.

Thomas P, Smart TG (2005) HEK293 cell line: a vehicle for the expression of recombinant proteins. J Pharmacol Toxicol Methods 51: 187–200.

Vaeth M, Yang J, Yamashita M, Zee I, Eckstein M, Knosp C, et al. (2017) ORAI2 modulates store-operated calcium entry and T cell-mediated immunity. Nat Commun 8: 14714.

Veschi EA, Bolean M, Strzelecka-Kiliszek A, Bandorowicz-Pikula J, Pikula S, Granjon T, et al. (2020) Localization of annexin A6 in matrix vesicles during physiological mineralization. Int J Mol Sci 21: 1367.

Wasilewska I, Gupta RK, Wojtas B, Palchevska O, Kuznicki J (2020) stim2b knockout induces hyperactivity and susceptibility to seizures in zebrafish larvae. Cells 9: 1285.

Wegierski T, Gazda K, Kuznicki J (2016) Microscopic analysis of Orai-mediated store-operated calcium entry in cells with experimentally altered levels of amyloid precursor protein. Biochem Biophys Res Commun 478: 1087–1092.

Wegierski T, Kuznicki J (2018) Neuronal calcium signaling via store-operated channels in health and disease. Cell Calcium 74: 102–111.

Weisz J, Uversky VN (2020) Zooming into the dark side of human annexin-S100 complexes: dynamic alliance of flexible partners. Int J Mol Sci 21(16) .

Williams RT, Manji SS, Parker NJ, Hancock MS, Van Stekelenburg L, Eid JP, et al. (2001) Identification and characterization of the STIM (stromal interaction molecule) gene family: coding for a novel class of transmembrane proteins. Biochem J 357: 673–685.

Zeng W, Yuan JP, Kim MS, Choi YJ, Huang GN, Worley PF, et al. (2008) STIM1 gates TRPC channels, but not Orai1, by electrostatic interaction. Mol Cell 32: 439–448.

Zhang H, Sun SY, Wu LL, Pchitskaya E, Zakharova O, Tacer KF, et al. (2016) Store-operated calcium channel complex in postsynaptic spines: a new therapeutic target for Alzheimer's disease treatment. J Neurosci 36: 11837–11850.